Since January 2020 Elsevier has created a COVID-19 resource centre with free information in English and Mandarin on the novel coronavirus COVID-19. The COVID-19 resource centre is hosted on Elsevier Connect, the company's public news and information website.

Sustainable Cities and Society 76 (2022) 103506

Contents lists available at ScienceDirect

Sustainable Cities and Society

journal homepage: www.elsevier.com/locate/scs

Examining spatiotemporal evolution of racial/ethnic disparities in human mobility and COVID-19 health outcomes: Evidence from the contiguous United States

Songhua Hu [a], Chenfeng Xiong [a,b,*], Hannah Younes [a], Mofeng Yang [a], Aref Darzi [a], Zhiyu Catherine Jin [a]

[a] Department of Civil and Environmental Engineering, Maryland Transportation Institute, University of Maryland, College Park, United States
[b] Shock Trauma and Anesthesiology Research (STAR) Center, School of Medicine, University of Maryland, Baltimore, United States

ARTICLE INFO

Keywords:
Racial/ethnic disparities
Human mobility
Non-pharmaceutical interventions
COVID-19
Mobile device location data
Generalized additive model

ABSTRACT

Social distancing has become a key countermeasure to contain the dissemination of COVID-19. This study examined county-level racial/ethnic disparities in human mobility and COVID-19 health outcomes during the year 2020 by leveraging geo-tracking data across the contiguous US. Sets of generalized additive models were fitted under cross-sectional and time-varying settings, with percentage of mobility change, percentage of staying home, COVID-19 infection rate, and case-fatality ratio as dependent variables, respectively. After adjusting for spatial effects, built environment, socioeconomics, demographics, and partisanship, we found counties with higher Asian populations decreased most in travel, counties with higher White and Asian populations experienced the least infection rate, and counties with higher African American populations presented the highest case-fatality ratio. Control variables, particularly partisanship and education attainment, significantly influenced modeling results. Time-varying analyses further suggested racial differences in human mobility varied dramatically at the beginning but remained stable during the pandemic, while racial differences in COVID-19 outcomes broadly decreased over time. All conclusions hold robust with different aggregation units or model specifications. Altogether, our analyses shine a spotlight on the entrenched racial segregation in the US as well as how it may influence the mobility patterns, urban forms, and health disparities during the COVID-19.

1. Introduction

The United States became a major epicenter of the Coronavirus disease 2019 (COVID-19) in 2020, reporting the greatest number of infections and fatalities worldwide (Dong et al., 2020). As a virus predominantly spread from person to person in close contact, substantial evidence has suggested that tailored public policies and well-designed built environment help control the spread of the virus, particularly when the mass deployment of effective vaccination has not been achieved yet (Hu et al., 2021; Kashem et al., 2021; Xiong et al., 2020). However, evidence also substantiates effects of countermeasures on curbing the spread of the virus are disproportionate, where socioeconomic status plays a critical role (Hooper et al., 2020; Johnson-Agbakwu et al., 2020; McLaren, 2020; Yancy, 2020). With more inequity being revealed, the COVID-19 has evolved into an unprecedented challenge involving social sustainability, structural equality, and health disparities. The pandemic creates a window of opportunity for achieving greater social resilience and sustainability in the construction of future healthy cities.

A range of control strategies has been conducted to slow the spread of the virus. Social distancing, i.e. staying home and away from others, is one of the key countermeasures through limiting physical movements and interactions (Flaxman et al., 2020; Fu & Zhai, 2021). Although studies have shown that social distancing can effectively flatten the spread of the virus (Noland, 2021; Xiong et al., 2020), evidence also suggests compounding structural inequalities in social distancing, where the racial/ethnic (abbreviated as racial) disparities play an important role (Chang et al., 2021; Hu et al., 2021; Jay et al., 2020; Sun et al., 2020; Weill et al., 2020). Meanwhile, racial disparities are among the strongest underlying factors associated with COVID-19 health outcomes

* Corresponding author.
E-mail addresses: hsonghua@umd.edu (S. Hu), cxiong@umd.edu (C. Xiong), hyounes@terpmail.umd.edu (H. Younes), mofeng@umd.edu (M. Yang), adarzi@umd.edu (A. Darzi).

https://doi.org/10.1016/j.scs.2021.103506
Received 22 June 2021; Received in revised form 20 September 2021; Accepted 22 October 2021
Available online 29 October 2021

in the US. Emerging data indicate that racial minorities, particularly African Americans (Abedi et al., 2021; Benitez et al., 2020; Devakumar et al., 2020; Yancy, 2020), bear a disproportionate burden of COVID-19 related outcomes. Such disproportion, also known as "epidemic injustice", has existed for a long time (Acevedo-Garcia, 2000) and can be traced back to the entrenched history of racial segregation in the US. Although de jure segregation has been outlawed since the 1960s, de facto segregation continues today in areas such as housing, occupation, and health care. Racial minorities in urban settings, whose socioeconomic statuses are systematically lower on average, disproportionately reside in overcrowded environments both by neighborhood and household assessments (Abedi et al., 2021; Hooper et al., 2020; Yancy, 2020). Meanwhile, they are more likely to engage in public-facing occupations that would be hard to contain social distancing during the pandemic (Benitez et al., 2020; Devakumar et al., 2020; Gross et al., 2020; Yancy, 2020). Research has also proven that in major US cities, hyper-segregated African Americans are more likely to be exposed to air pollutants, indicating a greater risk of disease (Zwickl et al., 2014). Understanding underlying mechanisms of such inequalities is critical to identify high-risk communities, tailor public policies, guide vaccine allocation, curb the spread of the virus, and ultimately, construct a more healthy, equal society.

Although racial disparities have been widely considered as the key factors associated with COVID-19 outcomes, it remains unclear whether racial disparities in social distancing have the same pattern as in COVID-19 health outcomes. This study aims to compare racial disparities in social distancing and COVID-19 health outcomes. Specifically, four questions are proposed. First, how to quantize the severity of COVID-19 health outcomes and the degree of compliance to social distancing by leveraging publicly available datasets? Second, how to simultaneously model social distancing and COVID-19 health outcomes under one framework with the control of their reverse causality? Third, how to adjust for confounding effects from other potential factors such as spatial effects, built environment, socioeconomics, demographics, and partisanship? And last, how to delineate the temporal evolution of racial disparities as the pandemic progressed?

To answer these questions, we assessed social distancing behaviors across more than 3000 counties in the contiguous US via two metrics: percentage of point-of-interest (POI) visit change using the year 2019 as the baseline (abbreviated as Pct. of visit change), and percentage of residents staying home (abbreviated as Pct. of staying home). We assessed county-level COVID-19 health outcomes via two metrics: number of cases per 100,000 population (abbreviated as cases/100,000), and number of deaths per 100 confirmed cases (aka case-fatality ratio, abbreviated as deaths/100 cases). Methodologically, we first depicted spatiotemporal distributions of the four metrics and calculated pairwise correlations between four metrics and various underlying factors. Then, we built several generalized additive models (GAMs) to examine the relationships between racial make-up and four metrics, respectively, successively controlling for other confounders. Last, we explored temporal evolutions of racial disparities by constructing sets of moving GAMs with dependent variables varying as their weekly average. For robustness check, we replicated the study at the census block group (CBG) level and tested a variety of model specifications. Our study shines a spotlight on racial segregation as well as how it may transfer to mobility changes and health disparities during the COVID-19. Our findings are expected to help inform the best practices to respond to the current COVID-19 pandemic and future epidemics that adequately account for health disparities and social equality across different socioeconomic communities. Policymakers and planners in the US should focus more on the racial segregation issue to promote health-related urban resilience, equality, and sustainability in the development of smart cities.

2. Literature review

2.1. Socioeconomic roots of COVID-19 health outcomes

Various studies have sought the socioeconomic roots of health disparities in COVID-19 by exploring the relationships between COVID-19 health outcomes and a range of exogenous factors, including socioeconomics, demographics, occupation, and living environment. Regions in low socioeconomic positions or with crowded living environments are more likely to present higher COVID-19 infection or death rates based on evidence from different US cities or other countries (Das et al., 2021; Kashem et al., 2021; Maiti et al., 2021). For example, one study in Chicago claimed that areas with low educational attainment consistently experienced higher case rates (Kashem et al., 2021). Similarly, another study explored the spatiotemporal effects of the driving factors on COVID-19 incidences in the contiguous US and stated that ethnicity, income, crime rate, and migration factors exhibited strong associations with COVID-19 cases and deaths (Maiti et al., 2021). Several studies analyzed the role of built and social environmental factors in COVID-19 transmission in Washington D.C. and King County, Washington stated that housing quality, race, and income present the strongest associations with the COVID-19 infections and deaths (Hu et al., 2021; Liu et al., 2021). Studies in other countries like Tehran, Brazil, and China also claimed that high population density and scarce medical service are the strongest predictors positively associated with COVID-19 infections and deaths (Lak et al., 2021; Li et al., 2021; Viezzer & Biondi, 2021; Wang et al., 2021).

In the US, racial disparities are among the strongest underlying factors associated with COVID-19 health outcomes (Liu et al., 2021; Maiti et al., 2021). Underrepresented minorities, particularly African Americans (Abedi et al., 2021; Almagro & Orane-Hutchinson, 2020; Benitez et al., 2020; Devakumar et al., 2020; Johnson-Agbakwu et al., 2020; Yancy, 2020) and Hispanics/Latinos (Almagro & Orane-Hutchinson, 2020; Benitez et al., 2020; Hooper et al., 2020), had disproportionately higher rates of COVID-19 infections and deaths. Latest studies further demonstrated that even after adjusting for extensive socioeconomics and pre-existing health issues, regions with more such underrepresented minorities still exhibited higher infection and fatality rates (Almagro & Orane-Hutchinson, 2020; McLaren, 2020).

2.2. Changes in human mobility during the pandemic

Previous studies have highlighted the importance and effectiveness of social distancing in slowing the spread of the virus (Noland, 2021; Xiong et al., 2020). Aided by continuously collected and widely covered location-based service (LBS) data, human mobility during the pandemic was successfully monitored (Grantz et al., 2020; Li et al., 2021; SafeGraph, 2020; Zhang et al., 2020) and was employed as a proxy of the degree of compliance to social distancing. During the pandemic, human mobility experienced dramatic but uneven changes across socioeconomic groups (Benita, 2021; Chang et al., 2021; Hu et al., 2021; Jay et al., 2020; Jiao & Azimian, 2021; Sannigrahi et al., 2020; Weill et al., 2020). One well-documented conclusion is that social distancing is a "privilege" for those in advantaged socioeconomic status (Fu & Zhai, 2021; Yancy, 2020). Regions with higher income, fewer essential workers, and higher flexibility of working from home, exhibited significantly higher decreases in mobility than their counterparts (Chang et al., 2021; Cuerdo-Vilches et al., 2021; Hu & Chen, 2021; Jay et al., 2020; Weill et al., 2020). In the US, partisanship is another salient factor related to social distancing. Republican-leaning counties exhibited substantially less social distancing than Democrat-leaning counties (Cai et al., 2021; Gollwitzer et al., 2020; Hu et al., 2021).

Although racial disparities also present strong associations with social distancing in the US, it is currently inconclusive on racial differences in mobility change. Some researchers emphasized African American-leaning regions did better in social distancing (Chiou & Tucker, 2020;

Garnier et al., 2021; Huang et al., 2020) while others claimed White-leaning regions performed better (Chang et al., 2021; Hu et al., 2021; Sy et al., 2020; Yancy, 2020). The underlying reason may be due to racial make-up, socioeconomics, and partisanship are always tangled. A well-designed model framework to disentangle their relationships is thus needed.

One current research gap is racial differences in human mobility and COVID-19 outcomes were analyzed separately. It remains unclear whether racial differences in human mobility correspond to the same pattern in COVID-19 health outcomes. Additionally, few studies have focused on the relationships between racial groups and other confounders like spatial effects, built environment, socioeconomics, demographics, and partisanship. Moreover, limited studies have analyzed the temporal evolution of racial differences across the entire year of 2020. Considering the declaration and lift of stay-at-home orders and the progressive shift of COVID-19 epicenters, understanding how racial differences vary throughout the pandemic is particularly important.

To fill these gaps, our analysis builds on previous work on human mobility and health outcomes during the pandemic by (1) focusing on the racial disparities during the pandemic by leveraging large-scale longitudinal human mobility and health data; (2) comparing the racial differences in human mobility and COVID-19 health outcomes; (3) successively controlling for extensive confounders to disentangle relationships among racial make-up and other underlying factors; (4) investigating the time-varying effects of racial make-up over the entire year of 2020; 5) conducting sufficient robustness checks on aggregation units and model specifications.

3. Data and variable description

3.1. Dependent variables

We examined human mobility in 3108 contiguous US counties during the year 2020 via percentage of visit change using the same week of the year 2019 as the baseline, and percentage of people staying home. For baseline design, unlike most previous studies using the pre-pandemic period in 2020 (Gollwitzer et al., 2020; Jay et al., 2020; Pullano et al., 2020), we employed the volume in 2019 to measure mobility change. Standardizing the human movement by volume in 2019 allows us to view variation in mobility more purely due to the pandemic, eliminating the natural variation (e.g. time-series seasonality, abnormal fluctuations) in mobility changes.

The two human mobility metrics were calculated using data from SafeGraph (SafeGraph, 2020), a data company that aggregates anonymized location-based service data from ~19 million smartphone devices observed per day across ~4.4 million POIs in the US. Specifically, we first used the Core Places US and Weekly Places Patterns (v2) datasets to calculate the county-level percentage change in visit frequency. These datasets contain hourly counts of visitors and geographical coordinates for each POI. We then used the Social Distancing Metrics v2.1, which contains daily estimates of the percentage of people staying home in each CBG. The staying-home devices are defined as those that stayed within ~150 m of their common nighttime locations throughout the day. All location data was de-identified and contains no private personal information. To avoid double-counting visits, we removed all parent POIs which include the visits from their child POIs (Chang et al., 2021). To address low-sample biases, we removed the records with an average sampling rate lower than 5% of the county population.

SafeGraph data has been used as one of the primary data sources in the US for tracking population flow during the COVID-19 pandemic (Chang et al., 2021; Fu & Zhai, 2021; Kashem et al., 2021). Previous studies have already conducted some data validation through the comparison with other mobility datasets, for instance, SafeGraph versus Google (Chang et al., 2021) and PlaceIQ (Weill et al., 2020). Their results showed that SafeGraph was highly consistent with other mobility data sources. In addition, SafeGraph has performed warranted analyses that suggest their data aligns with Census data (SafeGraph, 2020); for example, it does not systematically overrepresent or underrepresent individuals in counties with different racial make-ups. All geo-tracking data that support and validate the findings of this study are fully accessible from the SafeGraph website upon agreeing to certain sharing restrictions and ethics guidelines.

We assessed county-level COVID-19 outcomes via cases/100,000 and deaths/100 cases. The cases and deaths were from COVID-19 Data Repository by the Center for Systems Science and Engineering (CSSE) at Johns Hopkins University (Dong et al., 2020). Their dataset consists of cumulative counts of COVID-19 cases and deaths in the US over time at the daily county level.

3.2. Independent variables

Independent variables (Table 1) were selected based on well-documented evidence in previous literature (Abedi et al., 2021; Huet al., 2021; Jay et al., 2020; Xiong et al., 2020). Two sets of dependent variables were also mutually controlled to address the reverse causality (i.e. the simultaneity): when modeling human mobility, the cases/100,000 was controlled to capture panic effects of virus; when modeling COVID-19 outcomes, the percentage of visit change was controlled to capture mitigation effects of human mobility.

Our data on the racial make-up and socioeconomic factors came from the most recent 5-year (2015–2019) American Community Survey (ACS) of the US Census Bureau. We considered four main racial compositions: Non-Hispanic White (abbreviated as White, set as reference), Black/African American (abbreviated as African American), Hispanic/Latino (abbreviated as Hispanic), and Asian. Socioeconomics include (after variable selection): (1) Economic indices such as median household income, degree of income inequality (GINI coefficient), and percentage of residents with no health insurance coverage; (2) Demographic indices such as percentage of male, percentage of residents aged 65 years and over; (3) Built environment such as population density and rurality; (4) Occupations such as percentage of finance, percentage of administration, percentage of manufacturing, percentage of retail, percentage of transportation, percentage of educational services, percentage of healthcare, and percentage of accommodation and food.

Our data on partisanship was retrieved from the 2016 presidential election result provided by the MIT election lab (MIT, 2018). The percentage of total votes for Donald Trump was labeled as *Republican* and the percentage of total votes for Hillary Clinton was labeled as *Democrat*. We only included the *Democrat* in our model and set *Republican* as reference due to high multicollinearity. We also controlled for weather conditions including the differences in precipitation, wind speed, and minimum temperature between 2019 and 2020 using data from NOAA's National Centers for Environmental Information. More details regarding these variables and the descriptive statistics are provided in Table 1.

There is an important caveat here regarding the modifiable area unit problem (MAUP), which postulates that different regional aggregations of the units of observation may lead to different modeling estimations. This concern cannot be ignored especially in large US counties with significant racial residential segregation (Chen & Krieger, 2020). However, due to the unavailability of finer-grained data in both dependent variables (i.e. COVID-19 cases and deaths) and part of independent variables (e.g. GINI, partisanship, rurality), we employed the county as our spatial unit, which is the most granular data that we can currently obtain for all variables. For a robustness check, we partially conducted the research at the CBG level with variables that can be obtained at the CBG level (see Section 4.5).

4. Methods

The flowchart of research methodology is depicted in Fig. 1. We first analyzed the spatiotemporal distribution of human mobility and COVID-19 outcomes and checked their Moran's I statistics. We conducted

Table 1
Summary of county-level variables.

Variable		Description	Mean	St.d.	Median	Min.	Max.
Dependent Variable							
Pct. of visit change		Average percentage change in POI visits during 1 March to 31 December 2020, in%	−12.28	13.82	−11.01	−69.58	35.62
Pct. of staying home		Average percentage of people staying home during 1 March to 31 December 2020, in%	27.71	4.30	27.42	7.04	48.82
Cases/100,000		Cumulative number of COVID-19 cases per 100,000 population by the end of 2020, in count	6470.25	2788.98	6227.84	0.00	26,942.75
Deaths/100 cases		Cumulative number of COVID-19 deaths per 100 confirmed cases by the end of 2020, in count	1.80	1.14	1.56	0.00	12.00
Independent Variable							
Racial/ethnic groups	*White*	*The percentage of Non-Hispanic Whites, in%*	*76.59*	*19.88*	*83.88*	*0.69*	*99.59*
	African American	The percentage of African Americans, in%	9.16	14.57	2.34	0.00	87.23
	Asian	The percentage of Asians, in%	1.30	2.39	0.62	0.00	36.47
	Hispanic	The percentage of Hispanics/Latinos, in%	9.45	13.92	4.22	0.00	99.17
	Others	The percentage of other minorities including American Indian and Alaska Native alone, Native Hawaiian or other Pacific Islander, two or more races, and others, in%	6.24	8.27	3.93	0.00	94.78
Socio-economics	Finance	The percentage of finance and insurance, in%	3.30	1.63	2.99	0.00	18.79
	Scientific	*The percentage of professional, scientific, and technical services, in%*	*3.74*	*2.66*	*3.11*	*0.00*	*52.90*
	Administration	The percentage of administration, business support, and waste management services, in%	3.27	1.41	3.23	0.00	15.69
	Manufacture	The percentage of manufacturing industry, in%	12.34	7.09	11.42	0.00	46.39
	Retail	The percentage of retail trade and wholesale trade, in%	13.62	2.66	13.71	1.27	42.42
	Information	*The percentage of information, in%*	*1.33*	*0.80*	*1.25*	*0.00*	*11.61*
	Transportation	The percentage of transportation, warehousing, and utilities, in%	13.04	3.22	12.70	0.00	40.64
	Education	The percentage of educational services, in%	9.34	3.21	8.74	0.00	36.12
	Health Care	The percentage of healthcare and social assistance, in%	13.88	3.37	13.84	0.00	38.15
	Accommodation & Food	The percentage of accommodation, food, arts, entertainment, and recreation services, in%	8.31	3.60	7.95	0.00	41.37
	Agriculture	*The percentage of agriculture, forestry, fishing, hunting, construction, and mining, in%*	*13.95*	*7.55*	*11.96*	*0.90*	*61.47*
	GINI	A measure of statistical dispersion to represent the income inequality, from 0 (maximal inequality) to 1 (perfect equality)	0.45	0.04	0.44	0.32	0.71
	Median Income	The median household income (in 2019 Inflation-Adjusted Dollars), in $\$10^4$/household	5.33	1.41	5.17	2.15	14.23
	Poverty	*The percentage of households below national poverty level, in%*	*14.83*	*5.94*	*13.81*	*2.26*	*48.22*
	High Educated	*The percentage of residents with education attainment equal to/higher than Bachelor, in%*	*21.95*	*9.58*	*19.55*	*0.00*	*77.56*
	Without Insurance	The percentage of residents with no health insurance coverage, in%	9.55	4.98	8.65	0.67	40.91
	Total Population	*Total population, in 10^4*	*10.39*	*33.26*	*2.60*	*0.01*	*1008.16*
	Population Density	Population density, in 10^4 persons/sq. mile	0.03	0.18	0.00	0.00	7.20
	Central	1: Central (41.22%); 2: Outlying (17.78%); 3: Rural (41.00%)	–	–	–	–	–
	Work from Home	*The percentage of work-from-home commuters among workers 16 years and over, in%*	*5.09*	*3.18*	*4.44*	*0.00*	*34.11*
	Age over 65	The percentage of residents 65 years and over, in%	18.85	4.61	18.48	3.20	56.71
	Age 18–65	*The percentage of residents between 18 years and 65 years, in%*	*58.92*	*3.85*	*58.87*	*36.02*	*80.77*
	Age under 18	*The percentage of residents under 18 years, in%*	*22.23*	*3.46*	*22.24*	*7.27*	*41.80*
	Male	The percentage of male, in%	50.05	2.32	49.63	42.81	72.72
Partisanship	Democrat	The percentage of Democrats in 2016 presidential candidate vote totals, in %	31.50	15.19	28.28	3.14	90.86
	Republican	*The percentage of Republicans in 2016 presidential candidate vote totals, in%*	*63.28*	*15.64*	*66.34*	*4.09*	*96.03*
Weather	Precipitation	Difference in daily precipitation between 2019 and 2020, in mm	−0.24	0.86	−0.36	−2.68	2.86
	Wind Speed	Difference in daily wind speed between 2019 and 2020, in mph	0.08	0.31	0.07	−1.15	1.57
	Min. Temperature	Difference in daily minimum temperature between 2019 and 2020, in degrees F	0.39	0.66	0.25	−1.39	3.00

Notes: Dependent variables reported here are for the cross-sectional models. When fitting time-varying models, the dependent variables change to the corresponding weekly average. Variables in *Italic* were excluded from the models, either because of the high multicollinearity with other variables or the low capability in explaining the dependent variables.

pairwise analysis between all variables to understand their bivariate relationships. After preliminary analysis, we built a set of ordinary least-squares (OLS) regression to perform variable selection and model diagnostics. Based on diagnostic results, we modified our variable sets and model specifications, and fitted sets of cross-sectional models under the GAM framework. We further constructed sets of moving GAMs by allowing dependent variables to vary over time in order to examine temporal patterns of racial differences throughout the pandemic. Last, we replicated part of our analysis at the CBG level and tested other model specifications such as fixed-effect models and time-varying models under other time lags to check the robustness of our findings.

4.1. Variable selection and model diagnostics

Variable selection was performed to determine the optimal variable set. The variance inflation factor (VIF) was first calculated to test the multicollinearity, and VIFs greater than 5 were excluded. Then, a forward stepwise regression was employed to help select the independent variables based on the smallest AIC. Based on selected variables, we tested non-control OLS regression and diagnosed model assumptions including linearity, normality, homogeneity of residuals variance, and independence of residuals error terms (Supplementary Figs. S2,3). We also conducted the Moran's I test to check whether spatial autocorrelations are statistically significant in the four metrics as well as in their model residuals (Supplementary Fig. S4). In non-control models,

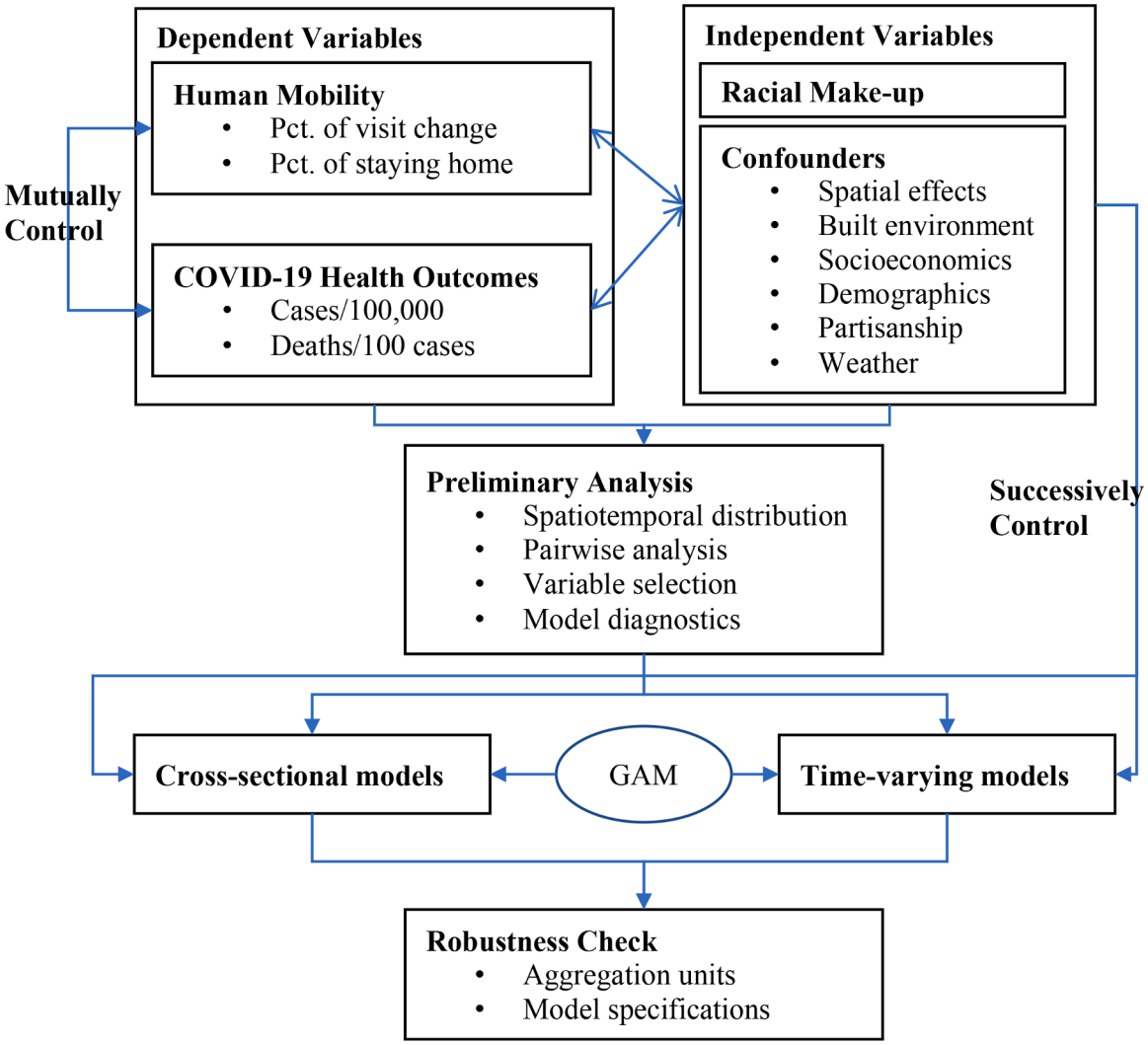

Fig. 1. Flowchart of research methodology.

Moran's I statistic varied from 0.269 to 0.605 with all P-value < 0.001, substantiating a statistically significant spatial clustering. After involving the spatial interaction, Moran's I decreased to 0.08 to 0.227, indicating the spatial autocorrelation in residuals has been largely eliminated.

4.2. Cross-sectional models with successive controls

The cross-sectional models were fitted under the generalized additive model (GAM) framework. GAM (Wood, 2003) is a semi-parametric model with a linear predictor involving a series of additive non-parametric smooth splines of covariates. Compared to the OLS linear regression, GAM is more flexible with fewer assumptions, which is useful when data fails to meet OLS assumptions, such as normality and homogeneity. Additionally, a noticeable advantage of GAM lies in its capability and flexibility to handle different nonlinear effects (Wood, 2003). By changing spline functions, various nonlinear effects can be fitted under one framework, such as random effects, nonlinear interactions, and spatial autocorrelations (Hu et al., 2021; Wang, Hu, & Jiang, 2020).

In our cases, the dependent variables in cross-sectional models included average percentage change in POI visits (V_i%), average percentage of people staying home (S_i%), total cases/100,000 (C_i), and total deaths/100 cases (F_i%) from 1 March to 31 December 2020, which are calculated as follows:

$$V_i\% = \frac{\sum_{t=9}^{T} v_{i,t} - \sum_{t=9}^{T} \ddot{v}_{i,t}}{\sum_{t=9}^{T} \ddot{v}_{i,t}}, S_i\% = \frac{\sum_{t=9}^{T} s_{i,t}}{\sum_{t=9}^{T} d_{i,t}} \quad (1)$$

$$C_i = 100,000 \frac{\sum_{t=9}^{T} c_{i,t}}{P_i}, F_i\% = \frac{\sum_{t=9}^{T} f_{i,t}}{\sum_{t=9}^{T} c_{i,t}} \quad (2)$$

where $v_{i,t}$ is the number of POI visits in county i during week t in 2020; $\ddot{v}_{i,t}$ is the number of POI visits in county i during week t in 2019; $s_{i,t}$ is the number of residents staying at home in county i in week t; $d_{i,t}$ is the number of observed devices in county i in week t; $c_{i,t}$ is the number of confirmed cases in county i in week t; $f_{i,t}$ is the number of deaths in county i in week t; P_i is the total population of county i.

When building GAMs, we first fitted a baseline OLS with no control Eq. (4)) and successively included state effects, socioeconomics, and partisanship (Eqs. (5)–((7)). Specifically, state effects include state random effects, weather conditions, spatial interaction, and simultaneity; socioeconomics include economic indices, demographic indices, built environments, and occupations. The formulations of the set of GAMs are as follows:

$$\frac{(Y_i - \mu_i)}{\sigma_i} \sim t(\vartheta_i), Y_i \in V_i, S_i, C_i, F_i \quad (3)$$

$$g(Y_i) = \beta_0^{(1)} + \sum_{r=1}^{R} \beta_r^{(1)} X_{r,i}^{(1)} + e_i \tag{4}$$

$$g(Y_i) = \beta_0^{(2)} + \sum_{r=1}^{R} \beta_r^{(2)} X_{r,i}^{(1)} + \delta^{(2)} K_i + f_l\left(X_{p,i} \times X_{q,i}\right) + R_i + W_i + e_i \tag{5}$$

$$g(Y_i) = \beta_0^{(3)} + \sum_{r=1}^{R} \beta_r^{(3)} X_{r,i}^{(1)} + \sum_{r=1}^{M} \gamma_r^{(3)} X_{r,i}^{(3)} + \delta^{(3)} K_i + f_l\left(X_{p,i} \times X_{q,i}\right) + R_i + W_i + e_i \tag{6}$$

$$g(Y_i) = \beta_0^{(4)} + \sum_{r=1}^{R} \beta_r^{(4)} X_{r,i}^{(1)} + \sum_{r=1}^{M} \gamma_r^{(4)} X_{r,i}^{(3)} + \alpha^{(4)} X_i^{(4)} + \delta^{(4)} K_i + f_l\left(X_{p,i} \times X_{q,i}\right) + R_i + W_i + e_i \tag{7}$$

$$K_i = I(Y_i \in V_i, S_i) C_i + I(Y_i \in C_i, F_i) V_i \tag{7}$$

where Y_i is one of the dependent variables from V_i, S_i, C_i, F_i, following scaled t-family with μ_i as expectation, σ_i as variance, ϑ_i as degree of freedom, and $g(.)$ is the link function; μ_i is determined by a linear predictor, while σ_i and ϑ_i are estimated alongside smoothing parameters; $\beta_0^{(1-4)}$ are the overall intercepts across models with different controls; $\beta_r^{(1-4)}$ are the coefficients of the r^{th} racial group $X_r^{(1)}$ across models with different controls, and R is the number of racial groups; $\gamma_r^{(3-4)}$ are the coefficients of the r^{th} socioeconomic features $X_r^{(3)}$ across models with different controls, and M is the number of socioeconomic features; $\alpha^{(4)}$ is the coefficient of partisanship $X^{(4)}$; K_i is the term to address the reverse causality, $I(.)$ is the indicator function, and $\delta^{(4)}$ is the corresponding coefficient; X_p and X_q are the pairs of independent variables nonlinearly interplaying with each other; $f_l(.)$ is marginal nonlinear smoother excluding the basic functions associated with the main effects (in our cases, the spatial coordinate interaction was fitted through this term); W_i is the weather conditions of county i; R_i is the nonlinear random effect of county i; e_i is the error term.

4.3. Time-varying effect models with moving dependent variables

We examined temporal evolutions of racial differences by constructing sets of GAMs under specifications similar to Eqs. (4)–(7), except that the dependent variables varied as their weekly average moving from week 1 to 52 in 2020. The COVID-19 outcome models were fitted only when the national cumulative case or death tolls were greater than 100. We also involved a two-week lag in human mobility when modeling COVID-19 outcomes (Eq. (12)) to capture the lagged effects of mobility change on curbing the transmission of virus (Gollwitzer et al., 2020; Xiong et al., 2020). We did not lag the COVID-19 outcomes when modeling human mobility (Eq. (12)) since the panic effects of virus on human behavior are immediate or preemptive (Huang et al., 2020). Other sizes of time lag were tested and found similar patterns (Supplementary Fig. S6).

The rationale behind the choice of time-moving regression instead of a longitudinal approach (e.g. a multi-level structure) is that almost all independent variables remain time-invariant during the pandemic. Moreover, panel models cannot discern the nonlinearity in time-varying effects, which is needed in understanding the coefficients' temporal evolution. In our cases, the formulations of four time-varying dependent variables are as follows:

$$V_{i,t}\% = \frac{v_{i,t} - \ddot{v}_{i,t}}{\ddot{v}_{i,t}}, S_{i,t}\% = \frac{s_{i,t}}{d_{i,t}} \tag{9}$$

$$C_{i,t} = 100,000 \frac{c_{i,t}}{P_i}, F_{i,t}\% = \frac{f_{i,t}}{c_{i,t}} \tag{10}$$

where $V_{i,t}, S_{i,t}$ are percentage of POI visit change and percentage of staying home in week t in county i; $C_{i,t}, F_{i,t}$ are number of COVID-19 cases/100,000 and deaths/100 cases in week t in county i; Other notations have the same meanings as in Eqs. (1)–(2).

The formulations of moving GAMs are similar to Eqs. (3)–(7). For brevity, here we only rewrite the formulations of fully-controlled models, i.e. the Eq. (7), in a time-varying setting (Eq. (11)). The reverse causality term (Eq. (12)) also changed into a lag format to capture lagged effects:

$$g\left(Y_{i,t}\right) = \beta_{0,t}^{(4)} + \sum_{r=1}^{R} \beta_{r,t}^{(4)} X_{r,i}^{(1)} + \sum_{r=1}^{M} \gamma_{r,t}^{(4)} X_{r,i}^{(3)} + \alpha_t^{(4)} X_i^{(4)} + \delta_t^{(4)} K_{i,t} + f_l\left(X_{p,i} \times X_{q,i}\right) + R_{i,t} + W_{i,t} + e_{i,t} \tag{11}$$

$$K_{i,t} = I\left(Y_{i,t} \in V_{i,t}, S_{i,t}\right) C_{i,t} + I\left(Y_{i,t} \in C_{i,t}, F_{i,t}\right) V_{i,t-u} \tag{12}$$

where $Y_{i,t}$ is one of the dependent variables from $V_{i,t}$, $S_{i,t}$, $C_{i,t}$, $F_{i,t}$, following scaled t-family with $g(.)$ as link function; $\beta_{0,t}^{(4)}$ is the overall intercept in week t; $\beta_{r,t}^{(4)}$ is the coefficient of the r^{th} racial group $X_r^{(1)}$ in week t; $\gamma_{r,t}^{(4)}$ are the coefficients of the r^{th} socioeconomic features $X_r^{(3)}$ in week t; $\alpha_t^{(4)}$ is the coefficient of partisanship $X^{(4)}$ in week t; K_t is the term to address the reverse causality in week t; u is the size of time lag (in week); $W_{i,t}$ is the weather conditions of county i in week t; $R_{i,t}$ is the random effect of county i in week t; $e_{i,t}$ is the error term; Other notations have the same meanings as in Eqs. (3)–(7).

5. Results

5.1. Spatiotemporal distribution

Fig. 2 illustrates the temporal evolution of human mobility and COVID-19 outcomes. Moving throughout the pandemic, we found human mobility plummeted steeply in March until reaching their nadir during late-April, followed by rapid recovery to near-unperturbed baseline in July; afterward, the gap between 2019 and 2020 in human mobility remained relatively stable until the end of 2020. Conversely, the percentage of staying home presented a reversed temporal pattern. Staying home percentage sharply increased from 24% to 37% in two months from March to late-April; after that, staying home percentage decreased and recovered to around 25% after July. The two health metrics, however, varied in substantially different patterns compared with human mobility. We noticed that there were three waves of epidemic outbreaks regarding the number of new confirmed cases, starting in May, August, and November, with each one higher than the previous. In addition, the temporal patterns of cases/100,000 and deaths/100 cases were not concurrent. The highest deaths/100 cases occurred in May, decreased afterward, and kept at a low rate regardless

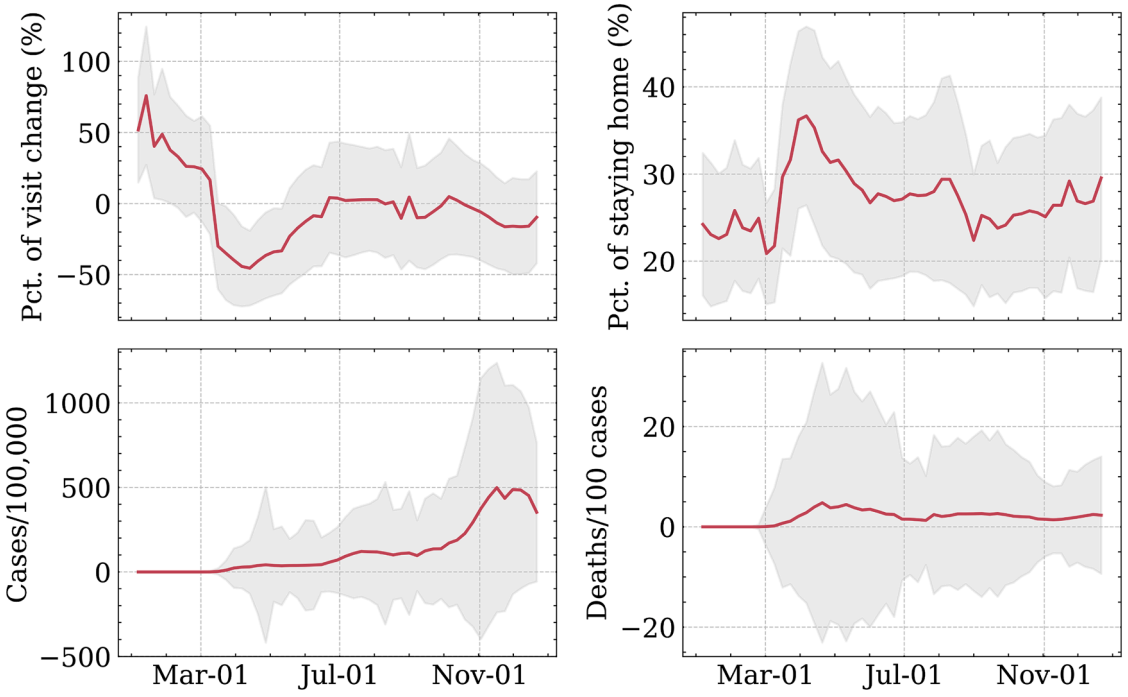

Fig. 2. Temporal evolution of human mobility and COVID-19 outcomes. Red curve represents the daily county-level average. Buffer denotes the county-level 95% CI (For interpretation of the references to color in this figure legend, the reader is referred to the web version of this article).

of the second and third waves of explosion of new confirmed cases. Such a pattern unravels the time-varying relationships among human mobility, COVID-19 outcomes, and other influential factors. We also noticed significant heterogeneity across different counties particularly in COVID-19 outcomes (the buffers in Fig. 2(b)), implying the necessity of adjusting for regional random effects when specifying models.

Fig. 3 shows the spatial distribution of four metrics in the contiguous US. We calculated the Moran's I statistics and found pronounced evidence of spatial clustering: Moran's I statistics are 0.564, 0.725, 0.567, and 0.321 for Pct. of visit change, Pct. of staying home, cases/100,000, and deaths/100 cases, respectively, with p-values all < 0.001. Such high spatial autocorrelation may be because non-pharmaceutical interventions and epidemic outbreaks were often targeted at an aggregate administrative level (Das et al., 2021). We further overlapped these metrics with the geographical distribution of racial make-up and observed distinguishable racial clustering, either manifesting as the spatial concentration within racial groups or the spatial exclusion among different racial groups (Supplementary Fig. S1). The salient spatial dependence corroborates the pronounced racial residential segregation in the US. It also suggests the necessity of controlling for spatial autocorrelation when fitting models.

5.2. Pairwise analysis

We calculated the pairwise correlation among variables and reported those ranking in the top 10 in terms of their correlations with dependent variables and racial groups (Table 2). We found partisanship (*Democrat* and *Republican*) presented the strongest correlation with two human mobility metrics, followed by *High Educated, Scientific, Asian*, and *Median Income*, all showing absolute Pearson coefficients greater than 0.4. Compared with human mobility metrics, COVID-19 outcome metrics presented lower correlations with independent variables. Cases/100,000 exhibited the strongest negative association with *Pct. of staying home*, followed by *Scientific, Administration*, and *High Educated*. Deaths/100 cases were negatively associated with *White* and *Median Income* and were positively associated with *African American* and *Poverty*.

Racial make-up was highly correlated with other controls, demonstrating high multicollinearity if we incorporated all variables into a model without preselection. We observed a significant and negative correlation between *White* and *Hispanic* as well as *White* and *African American*; hence, we excluded *White* from the model and set it as a reference. We also noticed *White* and *African American* were strongly associated with partisanship. Concretely, the correlation between *African American* and *Democrat* was markedly positive, as well as the correlation between *White* and *Republican*. However, the VIF test demonstrated acceptable values (i.e. VIF < 5) when one pair of race and partisanship coexisted, and we thus kept *African American* and *Democrat* in the final model. We also found *Asian* presented a pronounced and positive correlation with variables implying high socioeconomic status, for example, *Scientific, High Educated*, and *Median Income*. In contrast, *Hispanic* and *African American* exhibited a reverse pattern. *Hispanic* was positively correlated with *Without Insurance*, and *African American* was positively correlated with *Poverty*.

5.3. Cross-sectional modeling

Results of 16 cross-sectional models (4 metrics cross 4 sets of controls) were summarized in Table 3. Four sets of controls correspond to Eqs. (4)–(7), respectively, with racial coefficients corresponding to $\beta_r^{(1-4)}$. All variables were unstandardized for the convenience of interpretation. With the involvement of controls, the adjusted R-squared of four models were also enhanced, suggesting control variables did help in explaining the metrics. Moreover, the model goodness-of-fit of human mobility models were greater than the COVID-19 outcome models, with the deaths/100 cases model presenting the worst performance, indicating our independent variables were more related to human mobility compared with COVID-19 outcomes, which is also consistent with previous correlation analyses reported in Table 2.

The non-control models exhibited low model goodness-of-fit and unstable estimated associations. With the inclusion of controls, most racial associations flipped signs, changed magnitudes, or lost significance. Different sets of controls showed different effects on the racial coefficients. First, state effects substantially changed the magnitudes of relationships between all racial groups and *cases/100,000*, as well as

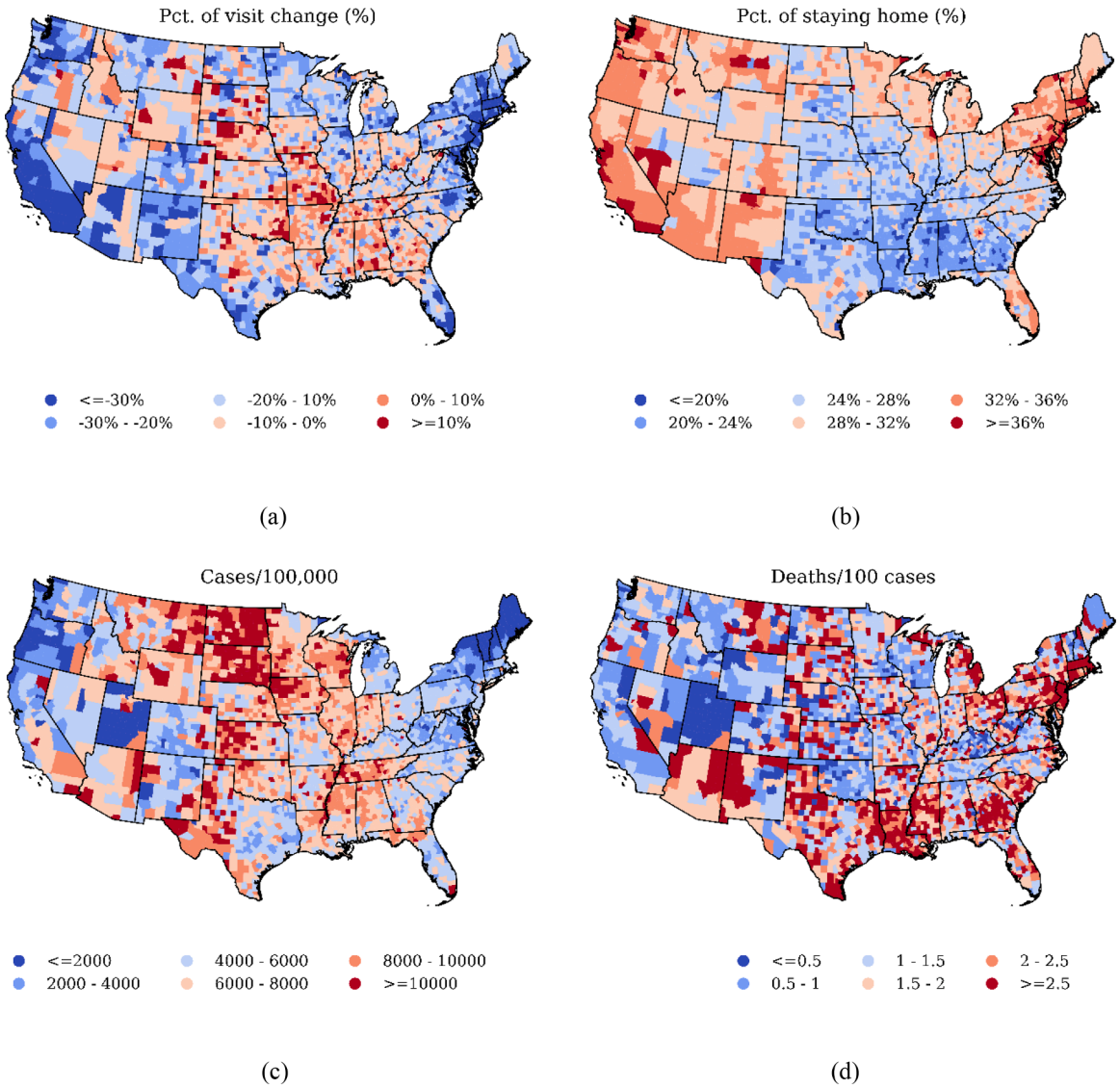

Fig. 3. Map of human mobility and COVID-19 outcomes in the contiguous US. Cooler and warmer colors imply less or greater value of metrics. More negative POI visit change and more positive staying home percentage imply more intensive compliance with social distancing. CBG-level maps for two human mobility metrics are available in Supplementary Fig. S7.

obscured the significance of relationships between all racial groups and *deaths/100 cases* except *African American*. Also, the model goodness-of-fit has been considerably improved after controlling for state effects, which may be attributed to the successful capture of nonlinear random effects across all states. Second, socioeconomics markedly influenced *Asian*, reducing the magnitudes of their relationships with two human mobility metrics, and magnifying the magnitudes of their relationships with *cases/100,000*. Socioeconomics also significantly reduced the relationships between *African American* and *cases/100,000*. Last, partisanship exerted the greatest effects on *African American*, changing the signs of their associations with human mobility metrics and magnifying the magnitudes of their relationships with *cases/100,000*. Partisanship also influenced *Asian* to some extent by obscuring the significance of their relationships with *cases/100,000*.

The final models (the last column in Table 3) documented the racial disparities as follows: during the pandemic, holding others constant and using White populations as reference, a county with 1% more African American populations was associated with a 0.06% (95% CI: 0.02, 0.10) augmentation in POI visits, 0.01% (95% CI: 0.00, 0.03) fewer residents staying home, 44.75 (95% CI: 36.34, 53.16) more cases/100,000, and 0.01 (95% CI: 0.01, 0.02) higher deaths/100 cases; a county with 1% more Hispanic populations was associated with a 0.12% (95% CI: 0.08, 0.15) reduction in POI visits, 0.03% (95% CI: 0.02, 0.04) more residents staying home, and 81.43 (95% CI: 73.07, 89.78) more cases/100,000; a county with 1% more Asian populations was associated with a 0.86% (95% CI: 0.64, 1.09) reduction in POI visits and 0.43% (95% CI: 0.37, 0.49) more residents staying home.

Altogether, our model suggested counties with higher Asian populations decreased most in human mobility, followed by Hispanic, White, and African American populations. This order did not hold accordingly regarding COVID-19 outcomes: counties with more White and Asian populations reported the least cases/100,000, followed by African American and Hispanic populations. Meanwhile, we found counties with more African American populations showed statistically significant higher deaths/100 cases even after adjusting for extensive confounding effects. For a robustness check, we tested other model specifications and found conclusions remained consistent when using state fixed effects instead of random effects (Supplementary Table S1) and when keeping influential outliers (Supplementary Table S2).

Table 2
Pearson correlation matrix for four metrics and four racial groups.

	Pct. of visit change		**Pct. of staying home**		**Cases/ 100,000**		**Deaths/100 cases**
Republican	0.668	Pct. of visit change	−0.637	Pct. of staying home	−0.309	African American	0.251
Pct. of staying home	−0.637	Republican	−0.546	Scientific	−0.307	White	−0.195
Democrat	−0.633	High Educated	0.505	Age under 18	0.268	Poverty	0.188
High Educated	−0.621	Scientific	0.502	Administration	−0.243	Median Income	−0.160
Scientific	−0.556	Democrat	0.481	High Educated	−0.225	GINI	0.157
Asian	−0.542	Asian	0.474	Male	0.214	Age over 65	0.147
Median Income	−0.475	Median Income	0.431	Pct. of visit change	0.210	High Educated	−0.146
Central	0.432	Total Population	0.354	Other minorities	0.189	Without Insurance	0.143
Age 18–65	−0.418	Central	−0.353	Accommodation & Food	−0.187	Age 18–65	−0.136
Total Population	−0.410	Cases/100,000	−0.309	Age over 65	−0.175	Population Density	0.129
	White		**African American**		**Asian**		**Hispanic**
Hispanic	−0.620	White	−0.619	Scientific	0.593	White	−0.620
African American	−0.619	Democrat	0.515	High Educated	0.563	Without Insurance	0.402
Democrat	−0.581	Poverty	0.444	Pct. of visit change	−0.542	Other minorities	0.313
Republican	0.526	Republican	−0.418	Total Population	0.533	Age under 18	0.313
Without Insurance	−0.506	GINI	0.386	Median Income	0.508	Manufacture	−0.264
Other minorities	−0.454	Work from home	−0.303	Pct. of staying home	0.474	Pct. of visit change	−0.262
Poverty	−0.415	Median Income	−0.257	Republican	−0.454	Age over 65	−0.237
Age over 65	0.383	Deaths/100 cases	0.251	Democrat	0.444	Agriculture	0.236
GINI	−0.356	Age 18–65	0.249	Population Density	0.366	Health Care	−0.223
Pct. of visit change	0.302	Agriculture	−0.248	Age 18–65	0.361	Total Population	0.193

Notes: All correlations have *P*-value < 0.001. Each column is ascendingly sorted by the absolute value accordingly.

Table 3
Results of cross-sectional GAMs with different sets of control variables.

Dependent Variable	**Race**	Non-control	Control: + State effects	Control: + Socioeconomics	Control: + Partisanship
Pct. of visit change (%)	African American	−0.02.(−0.05, 0.00)	−0.17*** (−0.20, −0.14)	−0.20*** (−0.23, −0.17)	0.06** (0.02, 0.10)
	Hispanic	−0.14*** (−0.17, −0.11)	−0.18*** (−0.21, −0.14)	−0.22*** (−0.25, −0.18)	−0.12*** (−0.15, −0.08)
	Asian	−4.49*** (−4.73, −4.25)	−3.59*** (−3.82, −3.36)	−1.13*** (−1.39, −0.87)	−0.86*** (−1.09, −0.64)
	Others	−0.10** (−0.16, −0.03)	−0.09*** (−0.15, −0.04)	−0.03 (−0.08, 0.02)	0.04 (−0.01, 0.09)
R^2 (Adjusted)		0.37	0.60	0.70	0.72
Pct. of staying home (%)	African American	−0.07*** (−0.08, −0.06)	0.03*** (0.02, 0.04)	0.04*** (0.04, 0.05)	−0.01* (−0.03, −0.00)
	Hispanic	0.00 (−0.01, 0.01)	0.03*** (0.02, 0.05)	0.05*** (0.04, 0.07)	0.03*** (0.02, 0.04)
	Asian	1.18*** (1.11, 1.26)	0.72*** (0.67, 0.78)	0.53*** (0.46, 0.59)	0.43*** (0.37, 0.49)
	Others	0.05*** (0.03, 0.07)	0.06*** (0.04, 0.07)	0.08*** (0.06, 0.09)	0.06*** (0.04, 0.07)
R^2 (Adjusted)		0.32	0.71	0.75	0.76
Cases/100,000	African American	4.55 (−1.59, 10.69)	20.77*** (15.27, 26.28)	8.41** (2.65, 14.18)	44.75*** (36.34, 53.16)
	Hispanic	10.47** (3.00, 17.95)	81.32*** (73.57, 89.06)	72.11*** (63.69, 80.54)	81.43*** (73.07, 89.78)
	Asian	−216.23*** (−260.36, −172.10)	−28.61. (−58.48, 1.26)	−51.43** (−84.49, −18.37)	−12.51 (−45.76, 20.75)
	Others	41.91*** (27.72, 56.09)	32.44*** (22.11, 42.78)	29.99*** (19.50, 40.49)	37.34*** (27.01, 47.68)
R^2 (Adjusted)		0.04	0.58	0.62	0.64
Deaths/100 cases	African American	0.02*** (0.02, 0.02)	0.01*** (0.01, 0.02)	0.01*** (0.01, 0.01)	0.01*** (0.01, 0.02)
	Hispanic	0.00* (0.00, 0.01)	−0.00 (−0.00, 0.00)	0.00 (−0.00, 0.01)	0.00 (−0.00, 0.01)
	Asian	−0.04*** (−0.06, −0.03)	−0.01 (−0.02, 0.01)	0.01 (−0.01, 0.02)	0.01 (−0.01, 0.02)
	Others	−0.01*** (−0.02, −0.01)	−0.00 (−0.01, 0.00)	−0.00 (−0.01, 0.00)	−0.00 (−0.01, 0.00)
R^2 (Adjusted)		0.08	0.26	0.32	0.32

Notes: Sets of controls were successively included as the analysis moves from one column to the next. Robust 95% confidence intervals are in parentheses. Significance codes: 0 '***' 0.001 '**' 0.01 '*' 0.05 '.' 0.1 ' ' 1.

5.4. Time-varying effects

Time-varying standardized coefficients of racial groups under different sets of controls were depicted in Fig. 4. Here we standardized the coefficients to help better compare among racial groups. Comparing across columns, we can observe how different sets of controls affected racial coefficients, which was consistent with the results shown in Table 3. In human mobility models (Fig. 4 rows 1 to 2), adjusting for socioeconomics substantially reduced the effects of Asian (columns 2 to 3, the red curve), while adjusting for partisanship reversed the signs of coefficients of *African American* (column 3 to 4, the blue curve). In COVID-19 models (rows 3 to 4), controlling for state effects markedly changed magnitudes of racial coefficients (columns 1 to 2). The number of weeks showing statistically significant racial coefficients with deaths/100 cases also greatly reduced after controlling for state effects (columns 1 to 2).

Our fully-controlled moving GAMs revealed that racial differences in human mobility experienced dramatic fluctuations at the beginning of the pandemic. Before the pandemic, counties with higher White populations exhibited the most human mobility. With the outbreak of the pandemic in March, coefficients of *African American* steeply flipped over the x-axis, indicating the ordering of mobility between White and African American populations was inverted. Such reversal was not observed between White and Asian or Hispanic populations. We also noticed in human mobility models that gaps in different racial coefficients reached the peak around mid-April; afterward, the gaps remained constant regardless of the nationwide lift of stay-at-home orders.

Temporal evolutions of racial coefficients in COVID-19 outcomes

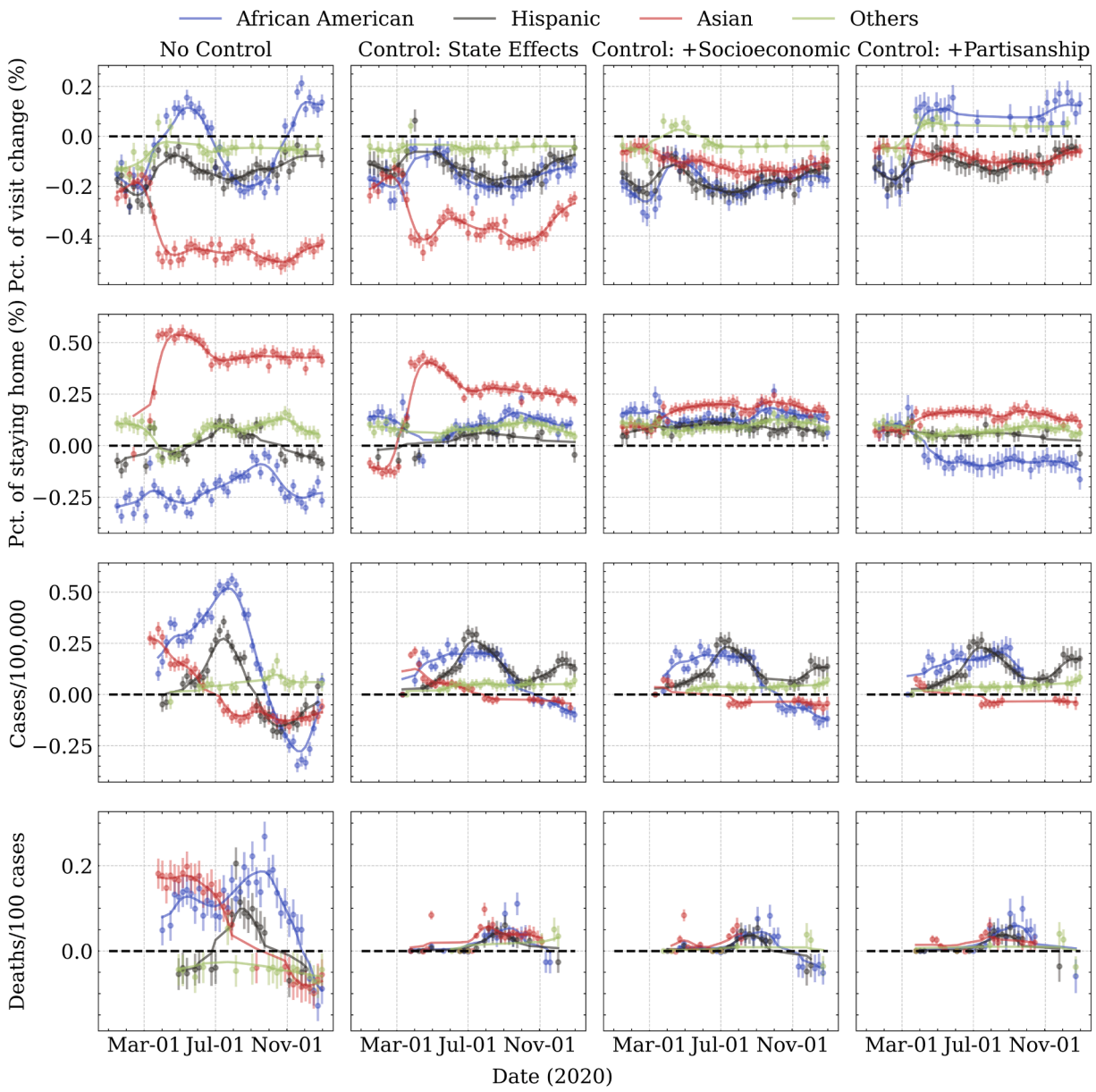

Fig. 4. Time-varying standardized coefficients of racial groups. Each row depicts one of the four metrics. Each column is a model successively controlling for sets of confounders. Each curve denotes the coefficient of one racial composition and is smoothed by the spline function. Only coefficients with *P*-values greater than 0.05 are plotted. Error bar depicts the robust 95% CI. Y-axis limits are shared by each row individually. The unstandardized version is reported in Supplementary Fig. S5 (For interpretation of the references to color in this figure, the reader is referred to the web version of this article).

were considerably different from those in human mobility. *African American* presented the strongest positive association with infection rate until July when the coefficient of *Hispanic* increased to a similar magnitude, followed by a decrease in coefficients of both *Hispanic* and *African American* until September, when coefficients of *African American* became insignificant while coefficients of *Hispanic* increased again until the end of 2020. We also observed that *Asian* only presented significantly positive relationships with COVID-19 outcomes in the early stage, while afterward, the relationships became insignificant or negative. Such change coincided with the shift of COVID-19 epicenters in the US from counties with higher African American and Asian populations to counties with higher Hispanic and White populations. Last, we observed a near 3-week time lag between temporal evolutions of *deaths/100 cases* and *cases/100,000*. For example, coefficients of *African American* in *cases/100,000* reached the highest in late-August, while in *deaths/100 cases* the peak occurred in mid-September; this is consistent with the average time from infection to death in prior epidemiological studies (Jung et al., 2020).

5.5. Modeling at census block group level

To explore the modifiable area unit problem, we conducted parts of our research at the CBG level, which is the smallest available spatial unit for which mobility data is available (Chang et al., 2021; Jay et al., 2020; Weill et al., 2020). As we did not have CBG-level COVID-19 cases and deaths, we only replicated two human mobility models (Supplementary Fig. S7). We also re-calculated the independent variables at the CBG level using the same datasets. Most independent variables were available at CBG-level, but some important variables were missing, including partisanship, rurality, GINI, and COVID-19 infections and deaths, which were filled by county-level attributes.

Results of CBG-level GAMs (Table 4) were broadly consistent with

Table 4
Results of cross-sectional models with different sets of controls (CBG level).

Dependent Variable	Race	No control	Control: + State effects	Control: + Socioeconomics	Control: + Partisanship
Pct. of visits change (%)	African American	−0.15***	−0.15***	−0.15***	−0.05***
		(−0.15, −0.14)	(−0.15, −0.14)	(−0.16, −0.15)	(−0.05, −0.04)
	Hispanic	−0.21***	−0.10***	−0.13***	−0.08***
		(−0.22, −0.20)	(−0.10, −0.09)	(−0.14, −0.13)	(−0.08, −0.07)
	Asian	−0.79***	−0.44***	−0.33***	−0.22***
		(−0.80, −0.78)	(−0.45, −0.43)	(−0.34, −0.32)	(−0.23, −0.21)
	Others	−0.14***	−0.08***	−0.08***	−0.04***
		(−0.15, −0.13)	(−0.09, −0.07)	(−0.09, −0.07)	(−0.05, −0.03)
R^2 (Adjusted)		0.15	0.25	0.30	0.33
Pct. of staying home (%)	African American	0.05***	0.08***	0.07***	0.05*** (0.05, 0.05)
		(0.05, 0.05)	(0.08, 0.08)	(0.07, 0.07)	
	Hispanic	0.04***	0.04*** (0.04, 0.04)	0.04***	0.03***
		(0.04, 0.05)		(0.04, 0.04)	(0.03, 0.03)
	Asian	0.28*** (0.28, 0.28)	0.21*** (0.21, 0.21)	0.19*** (0.19, 0.19)	0.17***
					(0.16, 0.17)
	Others	0.07***	0.04*** (0.04, 0.04)	0.04***	0.03***
		(0.07, 0.07)		(0.03, 0.04)	(0.03, 0.03)
R^2 (Adjusted)		0.23	0.43	0.46	0.48

Notes: This table is analogous to Table 3 human mobility part except the spatial unit is CBG.

county-level results in Table 3. Counties with higher Asian populations decreased most in human mobility, followed by Hispanic populations. However, the magnitudes of racial coefficients all decreased compared with county-level models, as well as the model goodness-of-fit. It is plausible since data with a finer-grained geographic unit contain more heterogeneity and randomness, which could increase the complexity of observed racial disparities. Another main difference was that after controlling partisanship, the association between *African American* and human mobility metrics did not flip the sign. In other words, CBG-level mobility models suggested that even after adjusting for partisanship effects, counties with higher White populations still performed the worst in following social distancing. The CBG-level time-varying coefficients further illustrated that African American-leaning counties only performed less social distancing than White-leaning counties in two months (from April to June 2020), while during the remaining periods, they performed more social distancing (Fig. 5). Such paradoxical findings, however, maybe because some important controls like partisanship, GINI coefficient, rurality, and COVID-19 outcomes were inaccessible at CBG-level. Thus, it would be inappropriate at this stage to claim the CBG-level model provided more reliable conclusions unless those CBG-level confounders were well controlled.

6. Discussion

This work leveraged large-scale location-based service data across ~4.4 million POIs in the contiguous US to characterize racial differences in human mobility and COVID-19 outcomes during 2020. After adjusting for various confounders, we found racial differences in human mobility and COVID-19 health outcomes presented different patterns. Counties with higher Asian populations exhibited the greatest social

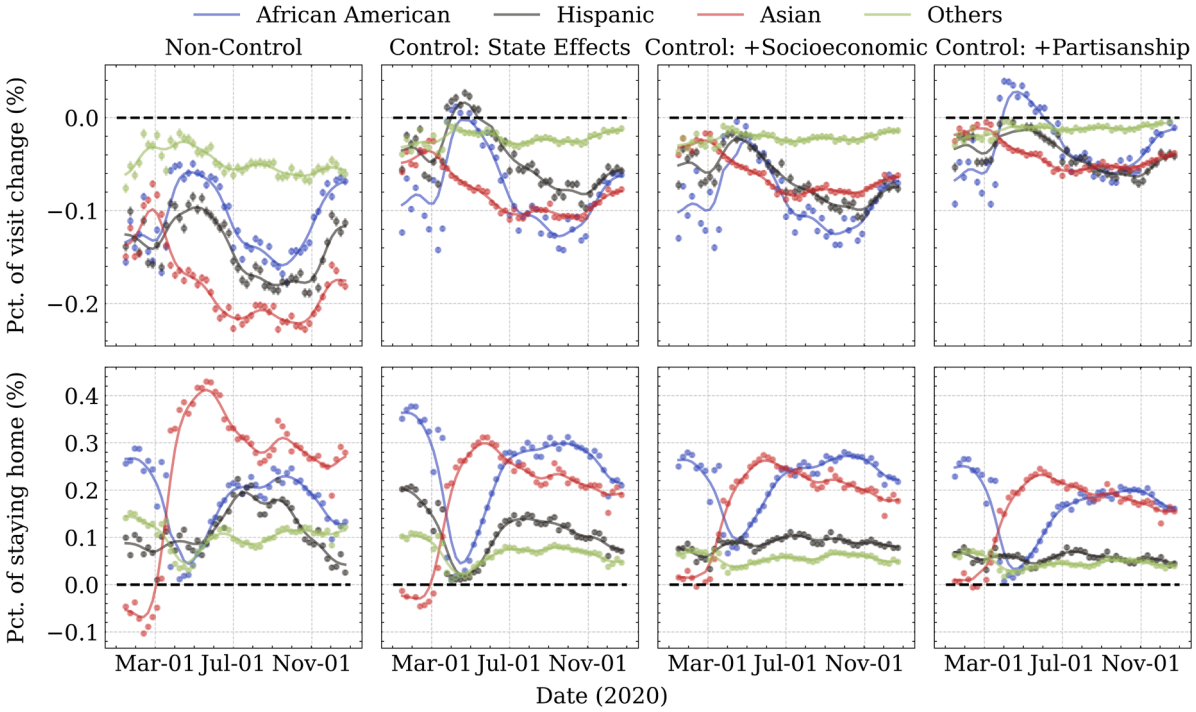

Fig. 5. Time-varying racial coefficients in fully-controlled models (CBG level). This figure is analogous to Fig. 4 row 1,2 in the main text except the spatial unit is CBG.

distancing, both in terms of reducing their overall movement and increasing their staying home percentage, followed by Hispanics, Whites, and African Americans. The same order did not hold accordingly in COVID-19 outcomes. Counties with higher White and Asian populations experienced the lowest infection rate, followed by African Americans and Hispanics. Counties with higher African American populations also exhibited the highest case-fatality ratio. The observed inconsistency, i.e. that counties with more racial groups who performed better social distancing did not always exhibit lower infection and case-fatality ratio, implies social distancing cannot fully explain the racial disparities in health outcomes. Other correlated factors, such as unobserved socioeconomic status and pre-existing health issues which have not been controlled in our models, may contribute to that inconsistency.

African Americans were the only group that presented a statistically higher case-fatality ratio than Whites even after adjusting for extensive controls, which was consistent with prior studies (Benitez et al., 2020; Hooper et al., 2020; McLaren, 2020; Yancy, 2020). Given that COVID-19 does not intrinsically discriminate across racial groups, reasons for such disparities remain up for debate. Unobserved disadvantaged socioeconomic status such as food insecurity and crowded living conditions; stark health inequities such as scarce testing and hospital resources; confluence of comorbidities such as hypertension, diabetes, and obesity; and deeply embedded systematic and structural racism, may all potentially account for such high case-fatality ratio (Abedi et al., 2021; Benitez et al., 2020; Devakumar et al., 2020; Gross et al., 2020; Hooper et al., 2020; Yancy, 2020). Specifically, disadvantaged communities of African Americans, which also happen to have the highest poverty rates (Table 2), are likely to own the fewest health resources and be the worst equipped for the pandemic (Abedi et al., 2021; Hooper et al., 2020; Yancy, 2020). High rates of underlying comorbidities among African Americans further exacerbate their vulnerability to COVID-19 (Benitez et al., 2020; Gross et al., 2020). Moreover, even those African Americans who possess high income, secure employment, good health status, and outstanding health insurance coverage still frequently receive inferior care due to implicit bias among healthcare providers (Devakumar et al., 2020).

Control variables also accounted for the differences in human mobility and COVID-19 outcomes. After controlling for partisanship, the association between African Americans and human mobility reversed the direction. Human mobility patterns in counties with more Democrats were opposite against counties with more African American populations, although Democrats and African Americans themselves were positively correlated. Counties with more Democrats presented significantly better social distancing. This partially explained why analysis without adjusting for partisanship displayed a better social distancing in African Americans-leaning counties (Chiou & Tucker, 2020; Papageorge et al., 2021): the better adherence may be due to the concentration of Democrats instead of only African Americans. In addition, socioeconomic features substantially influenced the coefficients of all racial groups; this is unsurprising since racial make-up and socioeconomics are closely intertwined and would jointly affect human mobility and COVID-19 outcomes. Pairwise correlation analysis further demonstrated that counties with high socioeconomic indicators such as high income, high rates of college education, and more scientific services, adhered better to social distancing; this supported findings in previous studies that higher socioeconomic position affords greater opportunity for people to adjust their travel behaviors during the pandemic (Jay et al., 2020; Maiti et al., 2021; Weill et al., 2020).

Time-varying coefficients demonstrated that racial differences in human mobility varied dramatically at the beginning of the COVID-19 but remained stable afterward, regardless of the progressive lift of stay-at-home orders. We documented a reversal in the ordering of human mobility between African Americans and Whites during the first wave of the outbreak. Before the pandemic, counties with higher White populations exhibited the highest mobility, while after the outbreak, counties with higher African American populations became the most mobile. Previous studies showed similar results stratified by income (Jay et al., 2020; Weill et al., 2020). Less mobility was associated with worse health outcomes before the pandemic due to physical inactivity and social isolation (Jay et al., 2020) but became a health-seeking behavior during the pandemic. Hence, the mobility inversion illustrated White-leaning counties tend to have greater autonomy to change their everyday mobility to achieve good health. The stable trend of racial differences in human mobility across the pandemic highlighted the voluntary nature of de-mobilizing behaviors, i.e. the reduction in movement was driven more by private initiatives, such as panic or social responsibility, rather than official directives, which is also in line with findings in prior studies (Hu et al., 2021). On the other hand, time-varying evolutions of coefficients in COVID-19 outcomes were considerably different from those in human mobility, which further demonstrated that the performance in social distancing could not be concurrently reflected in epidemic slowdown. Another important finding is, although the first wave of the outbreak occurred in counties with more African American and Asian populations, racial gaps in infection rates eventually disappeared as the pandemic progressed toward herd immunity (Fig. 4).

Findings from this study provide timely suggestions for pandemic control, urban planning, and social equality establishment. As the wooden bucket theory stated, the “shortest stave”, which are the most vulnerable populations in society, will eventually determine the overall resilience and robustness of a public health system. Hence, the most vulnerable group is suggested to be targeted as the highest priority in the allocation of protective gear, tests, and vaccines, which not only provides extra protection against the virus for those who are in imperative need, but also greatly allays the marginal risk of contagion for the rest of the population. Moreover, policymakers should focus more on measures that facilitate the implementation of social distancing among communities with high concentrations of racial minorities. Detailed policy options include enhancing the wage of essential jobs, dedicating information campaigns to increase awareness, providing safe mobility services to maintain connectivity between areas seeing sustained population flows, and mandating paid sick leave and work-from-home opportunities. Last, attention should be paid to those underrepresented minorities in the construction of city-level antivirus functions to increase social resilience and sustainability and prevent future virus like-attacks. Local governments and planners should use the current crisis to review how racial segregation systematically influences urban morphology. Efforts should be prioritized to socially vulnerable communities to increase their prevention ability and improve their living conditions, for example, instituting additional protection procedures, reallocating sufficient healthcare resources, decreasing housing density, and improving surrounding built environment and air quality.

7. Conclusions

Leveraging large-scale mobility and health data in 2020, this study compared and analyzed the racial differences in human mobility and COVID-19 health outcomes. Findings suggested vulnerable racial groups experienced substantially unequal risks of infection and death, which cannot be fully explained by well-documented determinants like human mobility, socioeconomic status, and partisanship. Time-varying effects further demonstrated racial differences in human mobility persisted regardless of the change in stay-at-home orders, while racial differences in COVID-19 health outcomes eventually disappeared as the pandemic progressed toward herd immunity. Considering the overall effectiveness in curbing the spread of the virus, social distancing is suggested to be strictly executed until most populations are successfully vaccinated. However, complementary policies are needed to help protect the most vulnerable and enhance policy efficacy. Efforts should also be made to the future construction of antivirus cities to increase health-related resilience, equality, and sustainability.

Several limitations are recognized and deserve further research.

First, variables used in our models are correlational and cannot prove causality. Second, all analyses were deduced at an aggregate level in the absence of available information at the individual level; hence, conclusions should not be extrapolated to individuals considering the possibility of the ecological fallacy. Third, our mobility data only represents the behavior of people with mobile devices who opt-in to location tracking, which may render sociodemographic and age biases — for example, underrepresentation of children and elderly (Grantz et al., 2020). Last, confirmed case and death counts of COVID-19 might not accurately reflect the real situation due to the inequitable distribution of testing resources and the exclusion of those ineligible patients who sought testing but symptoms did not meet the screening threshold.

Supplementary

Fig. S1. Map of human mobility and COVID-19 outcomes in the contiguous US. Each panel represents one metric from (a) average percentage change in POI visits from 1 March to 31 December 2020, (b) average percentage of people staying home from 1 March to 31 December 2020, (c) cumulative number of COVID-19 cases/100,000 by the end of 2020, and (d) cumulative number of deaths/100 cases by the end of 2020. Cooler and warmer colors indicate less or greater value of metrics.

Fig. S2. Linear regression diagnostics. Each panel represents one non-control linear model with four measures as dependent variables and racial make-up as independent variables. Figures in each panel represent the (1) Residuals vs Fitted plot; (2) Normal Q-Q plot; (3) Scale-location plot; (4) Residuals vs Leverage plot, respectively.

Fig. S3. Generalized additive model diagnostics. Each panel represents one fully-controlled linear model with four metrics as dependent variables. Figures in each panel represent the (1) Normal Q-Q plot; (2) Residuals vs Linear Fitted plot; (3) Histogram of residuals plot; and (4) Response vs. Fitted plot, respectively.

Fig. S4. Spatial distribution of residuals. Each panel represents residuals in models with four metrics as dependent variables. Figures in each panel represent the (1) residuals in non-control models (left) and (2) residuals in fully-controlled models (right), respectively.

Fig. S5. Unstandardized time-varying coefficients. This figure is analogous to Fig. 4 in the main text except the coefficients are unstandardized.

Fig. S6. Time-varying racial coefficients in fully-controlled models (3-weeks lag). This figure is analogous to Fig. 4 in the main text except the lag is 3 weeks instead of 2 weeks.

Fig. S7. Map of human mobility metrics in the contiguous US (CBG level). This figure is analogous to Fig. 3 (a,b) in the main text except the spatial unit is CBG level.

Table S1. Results of cross-sectional models with different sets of controls (Fixed effects)

Table S2. Results of cross-sectional models with different sets of controls (Raw data)

Declaration of Competing Interest

The authors have no conflict of interests to report.

Supplementary materials

Supplementary material associated with this article can be found, in the online version, at doi:10.1016/j.scs.2021.103506.

References

Abedi, V., Olulana, O., Avula, V., Chaudhary, D., Khan, A., Shahjouei, S., et al. (2021). Racial, economic, and health inequality and COVID-19 infection in the United States. *Journal of Racial and Ethnic Health Disparities, 8*(3), 732–742.

Acevedo-Garcia, D. (2000). Residential segregation and the epidemiology of infectious diseases. *Social Science & Medicine, 51*(8), 1143–1161.

Almagro, M., & Orane-Hutchinson, A. (2020). JUE insight: The determinants of the differential exposure to COVID-19 in New York city and their evolution over time. *Journal of Urban Economics*, Article 103293.

Benita, F. (2021). Human mobility behavior in COVID-19: A systematic literature review and bibliometric analysis. *Sustainable Cities and Society, 70*, Article 102916.

Benitez, J., Courtemanche, C., & Yelowitz, A. (2020). Racial and ethnic disparities in Covid-19: Evidence from six large cities. *Journal of Economics, 3*(4), 243–261. Race, and Policy.

Cai, S., Wang, X., Zhou, X., Hyman, M. R., & Yang, Z. (2021). Political and community logics jointly affect 'social distancing'compliance. *Sustainable Cities and Society, 74*, Article 103200.

Chang, S., Pierson, E., Koh, P. W., Gerardin, J., Redbird, B., Grusky, D., et al. (2021). Mobility network models of COVID-19 explain inequities and inform reopening. *Nature, 589*(7840), 82–87.

Chen, J. T., & Krieger, N. (2020). Revealing the unequal burden of COVID-19 by income, race/ethnicity, and household crowding: US county versus zip code analyses. *Journal of Public Health Management and Practice, 27*(1), S43–S56.

Chiou, L., & Tucker, C. (2020). *Social distancing, internet access and inequality*. National Bureau of Economic Research.

Cuerdo-Vilches, T., Navas-Martín, M.Á., March, S., & Oteiza, I. (2021). *Adequacy of telework spaces in homes during the lockdown in Madrid, according to socioeconomic factors and home features*. Sustainable Cities and Society, Article 103262.

Das, A., Ghosh, S., Das, K., Basu, T., Dutta, I., & Das, M. (2021). Living environment matters: Unravelling the spatial clustering of COVID-19 hotspots in Kolkata megacity, India. *Sustainable Cities and Society, 65*, Article 102577.

Devakumar, D., Shannon, G., Bhopal, S. S., & Abubakar, I. (2020). Racism and discrimination in COVID-19 responses. *The Lancet, 395*(10231), 1194.

Dong, E., Du, H., & Gardner, L. (2020). An interactive web-based dashboard to track COVID-19 in real time. *The Lancet Infectious Diseases, 20*(5), 533–534.

Flaxman, S., Mishra, S., Gandy, A., Unwin, H. J. T., Mellan, T. A., Coupland, H., et al. (2020). Estimating the effects of non-pharmaceutical interventions on COVID-19 in Europe. *Nature, 584*(7820), 257–261.

Fu, X., & Zhai, W. (2021). Examining the spatial and temporal relationship between social vulnerability and stay-at-home behaviors in New York City during the COVID-19 pandemic. *Sustainable Cities and Society, 67*, Article 102757.

Garnier, R., Benetka, J. R., Kraemer, J., & Bansal, S. (2021). Socioeconomic disparities in social distancing during the COVID-19 pandemic in the United States: Observational study. *Journal of Medical Internet Research, 23*(1), e24591.

Gollwitzer, A., Martel, C., Brady, W. J., Pärnamets, P., Freedman, I. G., Knowles, E. D., et al. (2020). Partisan differences in physical distancing are linked to health outcomes during the COVID-19 pandemic. *Nature Human Behaviour, 4*(11), 1186–1197.

Grantz, K. H., Meredith, H. R., Cummings, D. A., Metcalf, C. J. E., Grenfell, B. T., Giles, J. R., et al. (2020). The use of mobile phone data to inform analysis of COVID-19 pandemic epidemiology. *Nature Communications, 11*(1), 1–8.

Gross, C. P., Essien, U. R., Pasha, S., Gross, J. R., Wang, S.-Y., & Nunez-Smith, M. (2020). Racial and ethnic disparities in population-level Covid-19 mortality. *Journal of General Internal Medicine, 35*(10), 3097–3099.

Hooper, M. W., Nápoles, A. M., & Pérez-Stable, E. J. (2020). COVID-19 and racial/ethnic disparities. *JAMA, 323*(24), 2466–2467.

Hu, M., Roberts, J. D., Azevedo, G. P., & Milner, D. (2021). The role of built and social environmental factors in Covid-19 transmission: A look at America's capital city. *Sustainable Cities and Society, 65*, Article 102580.

Hu, S., & Chen, P. (2021). Who left riding transit? Examining socioeconomic disparities in the impact of COVID-19 on ridership. *Transportation Research Part D: Transport and Environment, 90*, Article 102654.

Hu, S., Xiong, C., Liu, Z., & Zhang, L. (2021). Examining spatiotemporal changing patterns of bike-sharing usage during COVID-19 pandemic. *Journal of Transport Geography, 91*, Article 102997.

Hu, S., Xiong, C., Yang, M., Younes, H., Luo, W., & Zhang, L. (2021). A big-data driven approach to analyzing and modeling human mobility trend under non-pharmaceutical interventions during COVID-19 pandemic. *Transportation Research Part C: Emerging Technologies, 124*, Article 102955.

Huang, V.S., .Sutermaster, S., Caplan, Y., Kemp, H., Schmutz, D., & Sgaier, S.K. (.2020). Social distancing across vulnerability, race, politics, and employment: How different Americans changed behaviors before and after major COVID-19 policy announcements. medRxiv.

Jay, J., Bor, J., Nsoesie, E. O., Lipson, S. K., Jones, D. K., Galea, S., et al. (2020). Neighbourhood income and physical distancing during the COVID-19 pandemic in the United States. *Nature Human Behaviour, 4*(12), 1294–1302.

Jiao, J., & Azimian, A. (2021). Exploring the factors affecting travel behaviors during the second phase of the COVID-19 pandemic in the United States. *Transportation Letters, 13*(5–6), 331–343.

Johnson-Agbakwu, C. E., Ali, N. S., Oxford, C. M., Wingo, S., Manin, E., & Coonrod, D. V. (2020). Racism, COVID-19, and Health Inequity in the USA: A Call to Action. *Journal of Racial and Ethnic Health Disparities*, 1–7. https://doi.org/10.1007/s40615-020-00928-y

Jung, S.-m., Akhmetzhanov, A. R., Hayashi, K., Linton, N. M., Yang, Y., Yuan, B., et al. (2020). Real-time estimation of the risk of death from novel coronavirus (COVID-19) infection: Inference using exported cases. *Journal of Clinical Medicine, 9*(2), 523.

Kashem, S. B., Baker, D. M., González, S. R., & Lee, C. A. (2021). Exploring the nexus between social vulnerability, built environment, and the prevalence of COVID-19: A case study of Chicago. *Sustainable Cities and Society*, Article 103261.

Lak, A., Sharifi, A., Badr, S., Zali, A., Maher, A., Mostafavi, E., et al. (2021). Spatio-temporal patterns of the COVID-19 pandemic, and Place-based influential factors at the neighborhood scale in Tehran. *Sustainable Cities and Society, 72*, Article 103034. https://doi.org/10.1016/j.scs.2021.103034

Li, B., Peng, Y., He, H., Wang, M., & Feng, T. (2021). Built environment and early infection of COVID-19 in urban districts: A case study of Huangzhou. *Sustainable Cities and Society, 66*, Article 102685.

Liu, C., Liu, Z., & Guan, C. (2021). The impacts of the built environment on the incidence rate of COVID-19: A case study of King County, Washington. *Sustainable Cities and Society, 74*, Article 103144.

Maiti, A., Zhang, Q., Sannigrahi, S., Pramanik, S., Chakraborti, S., Cerda, A., et al. (2021). Exploring spatiotemporal effects of the driving factors on COVID-19 incidences in the contiguous United States. *Sustainable Cities and Society, 68*, Article 102784.

McLaren, J. (2020). *Racial disparity in COVID-19 deaths: Seeking economic roots with census data.* National Bureau of Economic Research.

MIT, (2018). MIT election data, https://electionlab.mit.edu/data.

Noland, R. B. (2021). Mobility and the effective reproduction rate of COVID-19. *Journal of Transport & Health, 20*, Article 101016.

Papageorge, N. W., Zahn, M. V., Belot, M., Van den Broek-Altenburg, E., Choi, S., Jamison, J. C., et al. (2021). Socio-demographic factors associated with self-protecting behavior during the Covid-19 pandemic. *Journal of Population Economics, 34*(2), 691–738.

Pullano, G., Valdano, E., Scarpa, N., Rubrichi, S., & Colizza, V. (2020). Evaluating the effect of demographic factors, socioeconomic factors, and risk aversion on mobility during the COVID-19 epidemic in France under lockdown: A population-based study. *The Lancet Digital Health, 2*(12), e638–e649.

SafeGraph, (2020). SafeGraph data for academics, https://www.safegraph.com/academics.

Sannigrahi, S., Pilla, F., Basu, B., Basu, A. S., & Molter, A. (2020). Examining the association between socio-demographic composition and COVID-19 fatalities in the European region using spatial regression approach. *Sustainable Cities and Society, 62*, Article 102418.

Sun, Q., Zhou, W., Kabiri, A., Darzi, A., Hu, S., Younes, H. et al. (2020). COVID-19 and income profile: How people in different income groups responded to disease outbreak, case study of the United States. arXiv preprint arXiv:2007.02160.

Sy, K.T.L., Martinez, M.E., .Rader, B., & White, L.F. (.2020). Socioeconomic disparities in subway use and COVID-19 outcomes in New York City. MedRxiv.

Viezzer, J., & Biondi, D. (2021). The influence of urban, socio-economic, and eco-environmental aspects on COVID-19 cases, deaths and mortality: A multi-city case in the Atlantic Forest, Brazil. *Sustainable Cities and Society, 69*, Article 102859.

Wang, J., Yang, Y., Peng, J., Yang, L., Gou, Z., & Lu, Y. (2021). Moderation effect of urban density on changes in physical activity during the coronavirus disease 2019 pandemic. *Sustainable Cities and Society, 72*, Article 103058. https://doi.org/10.1016/j.scs.2021.103058

Wang, T., Hu, S., & Jiang, Y. (2020). Predicting shared-car use and examining nonlinear effects using gradient boosting regression trees. *International Journal of Sustainable Transportation, 15*(12), 893–907.

Weill, J. A., Stigler, M., Deschenes, O., & Springborn, M. R. (2020). Social distancing responses to COVID-19 emergency declarations strongly differentiated by income. *Proceedings of the National Academy of Sciences, 117*(33), 19658–19660.

Wood, S. N. (2003). Thin plate regression splines. *Journal of the Royal Statistical Society: Series B (Statistical Methodology), 65*(1), 95–114.

Xiong, C., Hu, S., Yang, M., Luo, W., & Zhang, L. (2020). Mobile device data reveal the dynamics in a positive relationship between human mobility and COVID-19 infections. *Proceedings of the National Academy of Sciences, 117*(44), 27087–27089.

Xiong, C., Hu, S., Yang, M., Younes, H., Luo, W., Ghader, S., et al. (2020). Mobile device location data reveal human mobility response to state-level stay-at-home orders during the COVID-19 pandemic in the USA. *Journal of the Royal Society Interface, 17*(173), Article 20200344.

Yancy, C. W. (2020). COVID-19 and african americans. *JAMA, 323*(19), 1891–1892.

Zhang, L., Ghader, S., Pack, M. L., Xiong, C., Darzi, A., Yang, M., et al. (2020). An interactive COVID-19 mobility impact and social distancing analysis platform. *medRxiv*.

Zwickl, K., Ash, M., & Boyce, J. K. (2014). Regional variation in environmental inequality: Industrial air toxics exposure in US cities. *Ecological Economics, 107*, 494–509.